THE JOURNAL OF PHYSICAL CHEMISTRY B

Article

pubs.acs.org/JPCB

Coarse-Grained Models for Aqueous Polyethylene Glycol Solutions

Eunsong Choi,[†] Jagannath Mondal,[‡,§] and Arun Yethiraj*[,‡]

[†]Department of Physics, and [‡]Department of Chemistry, University of Wisconsin, Madison, Wisconsin 53706, United States

ABSTRACT: A new coarse-grained force field is developed for polyethylene glycol (PEG) in water. The force field is based on the MARTINI model but with the big multipole water (BMW) model for the solvent. The polymer force field is reparameterized using the MARTINI protocol. The new force field removes the ring-like conformations seen in simulations of short chains with the MARTINI force field; these conformations are not observed in atomistic simulations. We also investigate the effect of using parameters for the end-group that are different from those for the repeat units, with the MARTINI and BMW/MARTINI models. We find that the new BMW/MARTINI force field removes the ring-like conformations seen in the MARTINI models and has more accurate predictions for the density of neat PEG. However, solvent-separated-pairs between chain ends and slow dynamics of the PEG reflect its own artifacts. We also carry out fine-grained simulations of PEG with bundled water clusters and show that the water bundling can lead to ring-like conformations of the polymer molecules. The simulations emphasize the pitfalls of coarse-graining several molecules into one site and suggest that polymer−solvent systems might be a stringent test for coarse-grained force fields.

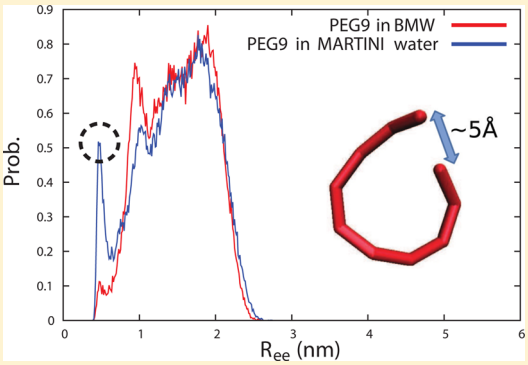

INTRODUCTION

Polyethylene glycol (PEG) is a water-soluble polymer that has considerable academic interest in addition to a variety of applications. For example, PEG can be attached to protein drugs to increase their circulating half-life and to reduce immunogenicity[1] and is used for bowel preparation prior to a colonoscopy.[2] It has often been used as a "crowding" agent in model studies of the effect of macromolecular crowding on protein folding and association rates.[3,4] It forms an aqueous two-phase system when mixed with dextran that shows promise for protein separation.[5] From a fundamental standpoint, it has been used to study the effect of depletion interactions on colloid stability.[6,7] The phase behavior is also interesting because it shows both a lower critical solution temperature (LCST) and an upper critical solution temperature (UCST) in experimentally accessible ranges of temperature.[8] The many applications and fundamental questions have motivated computational studies of this polymer, but the long length-scales of interest require a coarse-grained description. In this work, we develop a new coarse-grained model for PEG.

We study methyl-terminated PEG, which has the chemical formula:

$$CH_3{-}O{-}[CH_2{-}CH_2{-}O]_N{-}CH_3$$

where N is the degree of polymerization. For high molecular weights, $M_W > 3000$, these polymers are usually called polyethylene oxide or PEO,[9] but we will refer to the molecules as PEG regardless of molecular weight. The polymers can be terminated by either methyl or hydroxyl group, but we restrict our attention to the former.

A coarse-grained (CG) model of PEG/PEO has been developed by Lee et al.[10] within the MARTINI CG force-field framework; a sequence of three heavy atoms ($CH_2{-}O{-}CH_2$) was mapped to a single CG cite. The polymer molecule was solvated in MARTINI CG water,[25] and the parameters were adjusted to match experimental and all-atom simulation results. Conformation and hydrodynamic properties of high molecular weight chains (degree of polymerization $N > 67$) predicted by this CG model were in excellent agreement with all-atom simulations and experiments. However, despite this success for long chains, the CG model yielded unrealistic results for low molecular weight PEG. For example, the densities of low molecular weight neat PEG were overestimated (by up to 8%) as compared to the experimental observations. More interestingly, the end-to-end distance probability distribution function showed a sharp peak at low distances that (we show) corresponds to ring formation of the polymers, something that was not observed in atomistic simulations. We note that there are no experiments that rule out ring formation. PEG chains are known to associate end-to-end in the crystallization process, but ring formation is highly unlikely in short isolated chains, and is not seen in atomistic simulations. Another issue with the MARTINI model for PEG is the transferability of the force field. When the authors studied neat PEG or PEG in water,[10] they used a CG site of SNda type for the PEG monomer (we discuss the bead types in greater detail shortly). Yet when they studied the interaction of PEG with a dipalmitoylphosphatidylcholine (DPPC) membrane,[13] it was necessary to use a CG site of bead type SN0 for the PEG monomer.

Received: August 21, 2013
Revised: December 5, 2013
Published: December 18, 2013

Another MARTINI-based coarse-grained model of PEG has recently been developed by Rossi et al.[11] employing a new bead type coined P0. They used slightly smaller equilibrium values for bonds and angles to increase stabilities, which allowed them to use a larger time step (20 fs instead of 10 fs for neat PEG and dilute solutions). They used their model for the self-assembly of polyoxyethylene alkyl ether (C_iE_j) surfactants and did not study the conformational properties of PEG. Furthermore, given the interaction level between P0 beads, their model is expected to have the same problems for short chain PEG as the MARTINI model.

The fact that propensity for ring-like conformations decreases with increasing chain length suggests that this might be the end-effect, and we investigate treating the end-groups differently from the repeat units. It is well-known from theory[24] and experiment[9,33] that PEG with methyl-terminated end-groups displays phase behavior and thermodynamic properties different from those of PEG with hydroxyl-terminated end-groups. Although the difference between CH_3-O-CH_2(end-group) and CH_2-O-CH_2(repeat unit), is not expected to be nearly as significant, it might be important, especially for short chains. We investigate the use of bead types for the end-groups that are different from those for the repeat units in the hope of improving the force field for PEG oligomers. Although we find that the ring conformations have more to do with the solvent force field, the experimental densities of low molecular weight neat PEG can be accurately reproduced by using a more hydrophobic bead type for the end-group units.

The nonelectrostatic nature of the water model limits the applicability of the MARTINI model of PEG to more complex systems. It has been shown that the original MARTINI force field can be in qualitative error for several features such as adsorption of peptides to membranes, hydrophobic aggregation, and the phase behavior of lipid peptide mixtures. The big multipole water (BMW) model[14] was specifically designed to alleviate some of these problems with MARTINI, and the BMW/MARTINI force field (where lipid and peptide parameters are reparameterized with the BMW water) has been shown to be accurate for a number of physical phenomena, even for solutes that are not charged. For example, the association between hydrophobic peptides is predicted to be entropically driven in the BMW/MARTINI force field, consistent with experiment, while the original MARTINI or the MARTINI with polarizable water both predict that this association is enthalpically driven.[31]

In this Article, we develop a CG force field of (methyl-terminated) PEG using the BMW model for the solvent. We follow the same protocol as Lee et al.[10] for a parameterization of the force field. We show that the new force field reduces the error in the densities of low molecular PEG down to 1%, and greatly suppresses the formation of the ring conformation for short chains. We then discuss shortcomings of the new force field including the formation of the solvent-separated pair and slow dynamics. We also show that the use of the MARTINI polarizable water model[26] for the solvent does not yield any improvement over the standard MARTINI water.

SIMULATION DETAILS

All simulations are performed using GROMACS version 4.5.4.[15]

Coarse-Grained Simulations. Simulations are performed for single chains with N = 9, 18, 27, and 36, solvated in MARTINI, polarizable MARTINI (POL), and BMW water. For the four cases, 1072, 9499, 18 180, and 19 589 CG water molecules are used with MARTINI and POL water, and 2000, 9789, 12 865, and 26 065 water molecules are used with BMW water. The simulation cell is chosen large enough that a fully stretched chain will not interact with its periodic image. Initial configurations are created by inserting a fully stretched chain into the simulation cell followed by a steepest descent energy minimization to remove bad contacts between the sites. The temperature and pressure are kept at 296 K and 1 bar, respectively, using Berendsen's algorithm.[17] The system is propagated with a time step of 10 fs, and the total simulation time is 1 μs.

Simulations with MARTINI water and polarizable MARTINI water use a cutoff distance for the Lennard-Jones interaction of 12 Å with a smooth decay to zero between 9 and 12 Å. Electrostatic interactions for polarizable MARTINI water are calculated by using the Particle-Mesh-Ewald (PME) method[18,19] with a spacing of 0.2 nm, a real space cutoff distance 1.4 nm, and the dielectric constant ε_r = 2.5. Simulations with the BMW water do not use a cutoff,[14] and the Particle-Mesh-Ewald (PME) method is used with a spacing of 0.2 nm, a real space cutoff distance 1.4 nm, and the dielectric constant ε_r = 1.3 for the electrostatic interactions.

The trajectories are recorded every 10 ps, with the initial 10 ns used for equilibration. Properties are averaged over the remaining trajectory. Statistical uncertainties are determined by block averaging; the trajectory is divided into four blocks, and uncertainties are one standard deviation about the mean.

Fine-Grained Simulations. The OPLS force field[28−30] is used for atomistic simulations of PEG. A single chain with N = 9 is simulated with 880 bundled water molecules, which is equivalent to 3520 single point charge (SPC)[16] water molecules. For comparison, we also simulate PEG in SPC water, for which the simulation cell contains 4117 water molecules. A fully stretched single chain is solvated in the water box, and bad contacts are removed using a steepest descent minimization of the energy. The temperature and the pressure are kept at 296 K and 1 bar using Berendsen's algorithm. A time step of 2 fs is used, and the total simulation time is 100 ns. A cutoff distance for LJ interaction is set to 14 Å and smoothly decays to zero between 10 and 14 Å. The Particle-Mesh-Ewald (PME) method is used with a spacing of 0.12 nm and a real space cutoff distance 1.4 nm to calculate electrostatic interactions.

The trajectories are recorded every 2 ps, and initial 10 ns is used for equilibration. Properties are averaged over the remaining trajectory. Statistical uncertainties are determined by block averaging; the trajectory is divided into four blocks, and uncertainties are one standard deviation about the mean.

FORCE-FIELD PARAMETERIZATION

We parameterize force fields with BMW water, and with the end sites being different from the repeat units. We will refer to force fields without different end-groups FF1 and those with different end-groups FF2, with MAR referring to MARTINI water, POL referring to polarizable MARTINI water, and BMW referring to BMW water. The six force fields are therefore FF1-MAR, FF1-POL, FF1-BMW, FF2-MAR, FF2-POL, and FF2-BMW.

Parameterization of Force Field with BMW Solvent. We parameterize the CG force field of PEG in the BMW under the MARTINI force field[25] framework following the procedure

dx.doi.org/10.1021/jp408392b | J. Phys. Chem. B 2014, 118, 323−329

introduced by Lee et al.[10] In the MARTINI force-field framework, four heavy atoms are grouped into a single CG interaction cite. The CG interaction sites are characterized by four different bead types: polar (P), nonpolar (N), apolar (C), and charged (Q). Each bead type is further characterized either by a letter, for example, donor (d), acceptor (a), both donor and acceptor (da), or no hydrogen-bonding capability (0), or by a number in the range of 1−5, where 5 is the most polar and 1 is the least polar. Some CG sites map three heavy atoms instead of four, and these are denoted with the extra letter "S" in front of the bead type. For example, a CG bead type SNda indicates a three-heavy-atom site that is nonpolar and is both donor and acceptor. A Lennard-Jones (LJ) 12-6 potential is used for the non-bonded interaction between CG sites, with the effective size σ = 4.7 Å for four-heavy-atom cites and σ = 4.3 Å for three-heavy-atom cites. The LJ well depth ε is determined by the bead types of the interaction pair as defined in the interaction matrix presented in ref 25 with the extra scaling factor 0.75 for the interaction between S type sites.

In the development of FF1-BMW, the sequence of three heavy atoms (C−O−C) is mapped onto a single CG site. For an N-mer, there are therefore N+1 identical CG sites. (The end-group effect is treated in the FF2 force fields described in the next section.) The bead type is chosen to best reproduce the experimental density of low molecular weight neat PEG as well as the distributions of end-to-end distance and radius of gyration of single PEG chains from atomistic simulations. The SNa bead type underestimates the value of the root mean square end-to-end distance, R_{ee}, for N = 36, and we therefore choose the SP1 bead type, which gives results in better agreement with atomistic simulations. Note that, following the BMW/MARTINI protocol, all nonelectrostatic bead−water interactions are rescaled to reproduce relevant hydration and transfer energies.[32] As for the SP1 type beads, LJ well depth ε is rescaled to 75% of that in the MARTINI force field.

The bonded potentials are adjusted to match the distributions of bond lengths, bond angles, and dihedral angles with those seen in atomistic simulations[10] for N = 36. The form of these potentials is:

$$V_{\text{bond}}(b) = \frac{1}{2}K_b(b - b_0)^2 \quad (1)$$

$$V_{\text{angle}}(\theta) = \frac{1}{2}K_\theta(\theta - \theta_0)^2 \quad (2)$$

and

$$V_{\text{dihedral}}(\Phi) = \sum_{n=1}^{4} K_{\Phi,n}(1 + \cos(n\Phi - \Phi_n)) \quad (3)$$

The parameters in these potentials obtained after fitting to atomistic simulations, for the two force fields with the BMW solvent, are listed in the Summary of Force Fields.

Parameterization of End-Group Interactions. Although one expects the CH_3−O−CH_2 end-group and the CH_2−O−CH_2 repeat unit to be similar in terms of interactions, the results for short chains suggest that a slight difference could be significant. However, there is no clear guidance in how the potentials of interaction of these sites should differ. For example, while some united atom potentials have been parameterized for CH_3 and CH_2 groups,[21−23,27] with more strongly attractive interactions for the CH_3 groups, it is claimed in another study[24] that the CH_3 group is known to be more hydrophobic as compared to the repeat unit of PEG. In this work, we choose the CG sites to reproduce experimental data; a comparison with experimental data for the density of neat PEG shows that the FF1 force fields overestimate the density of short chains, with errors decreasing as the chain length is increased. This suggests that making the end-group more weakly interacting (more hydrophobic) than the repeat units should result in better agreement with the densities of neat PEG.

We find that using the SN0 bead type for the end-groups yields the best result when comparing simulations to experimental data for the density of neat PEG. Table 1 compares the densities of PEG obtained from the force-fields FF1 and FF2 to experimental data. The FF2 force fields reproduce the densities of neat PEG with an error of approximately 1% when compared to experiment, which is a significant improvement from the original FF1 force field, which overestimates the densities by as much as 8%. The distributions of the bond length, bond angles, and dihedral angles are virtually unaffected by the modified end-group units. The CG site types and intramolecular potential parameters are listed in the Summary of Force Fields.

Table 1. Densities of Low Molecular Weight PEG Obtained from the Original CG Force Field[10] without End Groups (FF1), Modified Force Field with End Groups (FF2), and Experiment[a]

	density (g/cm^3)			
N	FF1[10]	FF2-MAR	FF2-BMW	exp[10]
1	0.937	0.867	0.867	0.868
2	1.002	0.956	0.953	0.945
3	1.034	1.006	0.997	0.986
4	1.055	1.037	1.026	1.013
5	1.067	1.052	1.045	1.040

[a]Experimental densities are from the product data sheet, Ferro Fine Chemicals (as cited in Lee et al., 2009[10]).

Summary of Force Fields. We use the same intramolecular potentials for the FF1 and FF2 force fields because the end-group interactions have no discernible effect on distributions of bond lengths, bond angles, and dihedral angles. The parameters are b_0 = 3.3 Å, K_b = 17 000 kJ/mol, θ_0 = 128°, and K_θ = 35 kJ/mol. The parameters for the dihedral potential are listed in Table 2. The bead types in the different force fields are listed in Table 3. Note that the parameters for the CG PEG in the polarizable MARTINI water are the same as those in the standard MARTINI water; that is, it was not necessary to reparameterize the MARTINI bead types for the POL water.

Table 2. Bonded Potential Parameters for PEG with the BMW Solvent[a]

n	ϕ_n (deg)	$K_{\phi,n}$ (kJ mol^{-1})
1	180	1.80
2	0	−0.40
3	0	−0.20
4	0	0.30

[a]The parameters for the force fields in the MARTINI water can be found in ref 10.

dx.doi.org/10.1021/jp408392b | J. Phys. Chem. B 2014, 118, 323−329

Table 3. CG Bead Types Defined under the MARTINI[25] Force Field and under the BMW-MARTINI[32] (Denoted by the Asterisk) Force Field

	FF1-MAR[10]	FF1-BMW	FF2-MAR	FF2-BMW
CH_2-O-CH_2	SNda	SP1*	SNda	SNa*
CH_3-O-CH_2	SNda	SP1*	SN0	SN0*

RESULTS AND DISCUSSION

All six force fields reproduce the bond length, bond angle, and dihedral angle distributions observed in atomistic simulations. Figure 1 compares results from the CG force fields to results

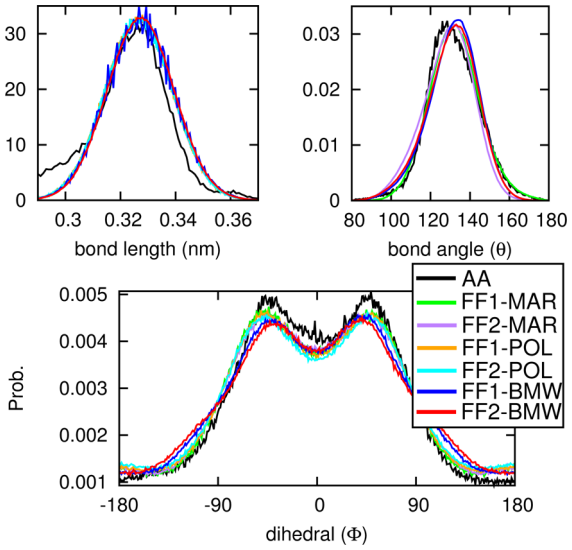

Figure 1. Comparison of distributions of bond length, bond angle, and dihedral angles from the CG force fields to atomistic simulations[10] for $N = 36$.

from atomistic simulations for $N = 36$. Of course, the parameters were fit to reproduce these distributions for short chains, so this is not a test of the force fields. Rather the agreement in Figure 1 and Table 1 suggests that the force field parameterization was successful given the chosen protocol.

The CG force fields are all in good agreement with atomistic simulation results[10,12] for the average chain size, characterized by the root-mean-square radius of gyration, R_g, or the root-mean-square end-to-end distance, R_{ee}. Tables 4 and 5 list R_g and R_{ee} values from the different models for $N = 9$, 18, 27, and 36. The agreement with atomistic simulations is poorer for $N = 18$ than the other chain lengths, a feature we do not have an explanation for.

Table 4. Comparison of CG Predictions for the Root Mean Square Radius of Gyration, R_g, to Atomistic Simulations

	R_g (Å)			
	PEG9	PEG18	PEG27	PEG36
FF1-MAR	6.3 ± 0.1	9.0 ± 0.3	10.9 ± 0.9	12.9 ± 0.3
FF2-MAR	6.3 ± 0.1	9.4 ± 0.1	11.2 ± 0.2	12.0 ± 0.3
FF1-POL	6.3 ± 0.2	8.4 ± 0.1	11.8 ± 0.2	13.3 ± 0.2
FF2-POL	6.4 ± 0.1	9.6 ± 0.1	12.0 ± 0.2	13.9 ± 0.4
FF1-BMW	6.3 ± 0.1	9.1 ± 0.3	11.4 ± 0.7	13.2 ± 0.5
FF2-BMW	6.3 ± 0.1	9.3 ± 0.1	11.3 ± 0.2	13.3 ± 0.2
atomistic[10]	6.4 ± 0.1	8.8 ± 0.2	11.2 ± 0.3	13.2 ± 0.5

Table 5. Comparison of CG Predictions for the Root Mean Square End-to-End Distance R_{ee} to Atomistic Simulations

	R_{ee} (Å)			
	PEG9	PEG18	PEG27	PEG36
FF1-MAR	15.9 ± 0.3	21.7 ± 1.5	25.8 ± 3.5	31.2 ± 0.7
FF2-MAR	16.0 ± 0.1	23.8 ± 0.3	27.4 ± 0.7	30.0 ± 0.9
FF1-POL	15.8 ± 0.1	23.6 ± 0.2	29.7 ± 0.5	33.4 ± 0.5
FF2-POL	16.2 ± 0.1	24.4 ± 0.5	30.5 ± 0.7	35.8 ± 1.3
FF1-BMW	15.7 ± 0.4	21.6 ± 1.6	27.3 ± 3.2	31.9 ± 2.5
FF2-BMW	15.6 ± 0.4	22.9 ± 0.4	27.0 ± 0.8	32.4 ± 0.8
atomistic[10]	15.5 ± 0.4	20.0 ± 0.7	27.6 ± 1.4	32.1 ± 2.2

The ring-like conformations (manifested in a peak in the distribution of end-to-end distance R_{ee}) are absent with the BMW force fields. Figure 2 depicts the end-to-end distance

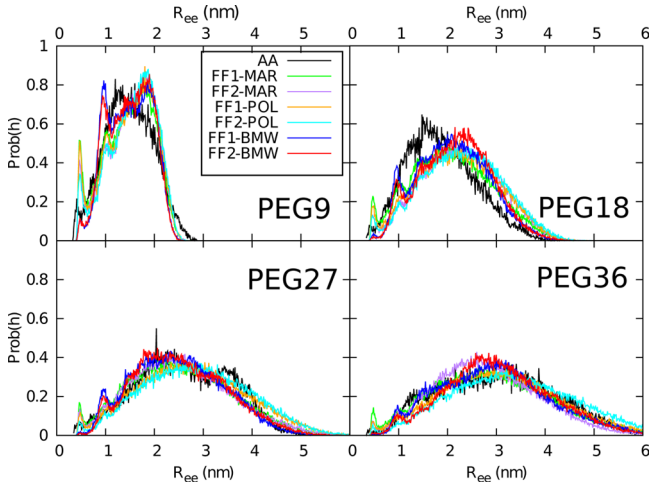

Figure 2. Distributions of the end-to-end distance R_{ee} from the different force fields. Atomistic simulation results are obtained from Lee et al.[10]

distribution for $N = 9$, 18, 27, and 36. For the longest chain, all of the force fields are in good agreement with results of atomistic simulations[10,12] except that the MARTINI force fields have a small peak at $R_{ee} \approx 5$ Å, which is absent in the atomistic simulations. Note that the size of the peak in FF2-MAR force field does not change much when compared to that of FF1-MAR, meaning the use of less attractive end beads does not have a significant effect. As the chain length is decreased, this peak becomes more prominent in all of the MARTINI force fields. We also note that the results using the MARTINI force field with POL water are almost identical to those using the standard MARTINI water. Interestingly, the peak at $R_{ee} \approx 5$ Å is absent in the BMW force fields, but the BMW force fields introduce another, albeit less prominent, peak at $R_{ee} \approx 10$ Å. This peak indicates the formation of the solvent-separated ring in the BMW/MARTINI force field and is consistent with the potential of mean force (PMF) between uncharged molecules in BMW recently reported by Wassenaar et al.[34] where a global minimum is found at a distance ~1 nm. (Representative snapshots of the two peaks are shown in Figure 3.)

What is the origin of the "ring" peaks seen in the CG force fields? Why do MARTINI and BMW/MARTINI force fields form different ring conformations? Because the various trial force fields failed to remove the ring-like conformations or at best suppressed them only to some degree, the preference

dx.doi.org/10.1021/jp408392b | J. Phys. Chem. B 2014, 118, 323−329

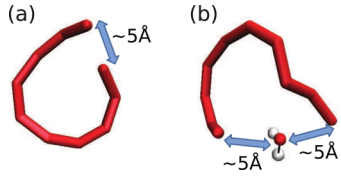

Figure 3. Representative snapshots of (a) a ring conformation ($R_{ee} \approx$ 5 Å) in the MARTINI and (b) a solvent-separated-ring conformation ($R_{ee} \approx$ 10 Å) in the BMW. The snapshots are generated by using VMD.[35]

toward the ring-like conformations is likely a coarse-graining artifact rather than a consequence of unrealistic force-field parameters. In particular, the idea of mapping four water molecules into a single CG site is questionable because there is no corresponding constraint that keeps a group of water molecules together in real water systems. To investigate this further, we study an atomistic model of water where four water molecules are bundled together using harmonic springs.

We follow the strategy introduced by Fuhrmans et al.[20] to bundle SPC water into groups of four. The liquid is grouped into sets of four water molecules, and in each set a harmonic "intramolecular" bundling potential is applied between the oxygen atoms. The bundling potential is

$$V_{\text{bundling}} = \begin{cases} \frac{1}{2}k_{\text{dr}}(r_{ij} - 0.3)^2 & \text{if } r_{ij} > 0.3 \text{ nm} \\ 0 & \text{otherwise} \end{cases} \quad (4)$$

where r_{ij} is the distance between oxygen atoms measured in nm and k_{dr} = 1000 kJ mol^{-1}nm^{-2}. The bundling potential is turned off for r_{ij} < 0.3 nm to minimize artifacts at short distances; the equilibrium distance between neighboring water molecules is about 0.28 nm. The non-bonded potential between water molecules is adjusted to ensure that the nearest neighboring water molecules are intramolecular ones while leaving the overall density unchanged (the details can be found in in the original paper[20]). Note that because the bundling potential (eq 4) is applied symmetrically between all intramolecular oxygen pairs, the resulting structure of a bundled water molecule is tetrahedral.

Figure 4 compares the distribution of end-to-end distance from simulations of an atomistic model of PEG, with SPC water and bundled SPC water, for N = 9. (For easier comparison with the CG simulations, the center-of-mass of the CH_3-O-CH_2 group is used as the end of the chain.) We

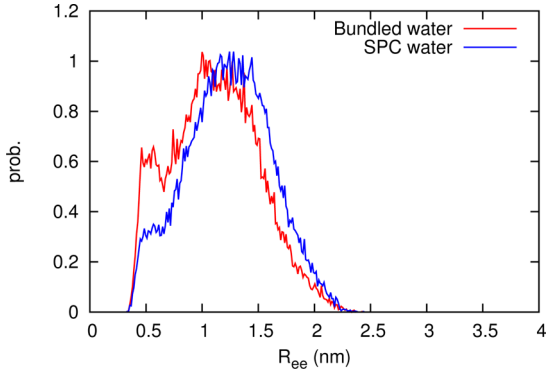

Figure 4. Distributions of the end-to-end distance R_{ee} for N = 9 in the SPC water and in the bundled SPC water.

use the OPLSAA force field[28−30] for the PEG chain. A peak at $R_{ee} \approx$ 5 Å is seen in the bundled water simulations, just as in the MARTINI models. The origin of the peak therefore lies purely in the bundling of the four water molecules with the harmonic potential because there are no other differences between the SPC and bundled SPC simulations; for example, the chain is treated atomistically in both cases.

The reason for the difference between BMW and MARTINI water in predictions for ring structure can be inferred from the way the BMW model is developed. The BMW is parameterized to reproduce the mean electrostatic properties of (unbundled) water clusters.[14] Because clusters break and regroup and can penetrate one another, the BMW model does not represent bundles of water molecules. In some sense, MARTINI corresponds to dividing the water molecules into groups of four (as in bundled water), while BMW corresponds to dividing space into water clusters. This may be the reason the BMW does not predict the peak that is observed in the MARTINI and in the bundled water simulations. On the other hand, the solvent-separated ring found in the BMW simulations probably has a different origin. Although we do not have a clear explanation, asymmetrically applied soft interaction,[14] soft BMH potential between solvents but normal LJ potential between all others, could be one reason. As mentioned above, the preferred formation of the solvent-separated pair that we observe is consistent with the recently reported PMF calculations.[34] It is shown that the global minimum in PMF between various uncharged molecules in the BMW is located at a distance near 1 nm. Our result also confirms the strong preference toward the formation of the solvent-separated pair (the $R_{ee} \approx$ 1.0 nm peak) between solutes in the BMW.

Apart from the solvent-separated ring conformation observed in the BMW force fields, another shortcoming of the new model is its slow dynamics. In Figure 5, we show self-diffusion

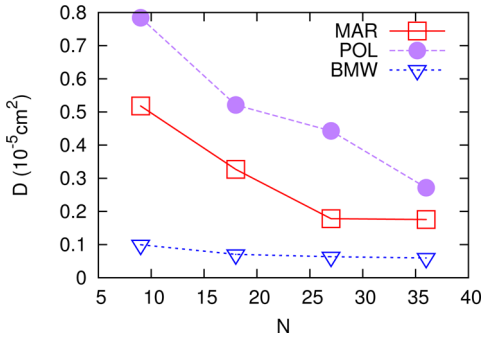

Figure 5. Self-diffusion coefficients of PEG in three different solvent models as a function of degree of polymerization N. Lines are to guide the eyes. The FF1 force field is used for the standard MARTINI water (MAR) and the polarizable water (POL), and the FF2 force field is used for the BMW, but there is no noticeable difference between FF1 and FF2 for BMW in terms of diffusion coefficients.

coefficients of PEG using different solvent models. Among all three force fields, the diffusion constant is highest in the POL and lowest in the BMW, with MAR between. Slow dynamics essentially means inefficient sampling through the phase space, which would increase the computational burden, making the BMW model less useful when the system size is large.

dx.doi.org/10.1021/jp408392b | J. Phys. Chem. B 2014, 118, 323−329

SUMMARY AND CONCLUSIONS

We present coarse-grained force fields for methyl-terminated PEG molecules in water. Our development is based on the MARTINI approach introduced by Lee and coauthors,[10] but we include an explicit description of solvent electrostatics, via the BMW model for the solvent, and a treatment of the end-groups with different parameters from the repeat units. The new model predicts more accurate densities of low molecular weight neat PEG and removes the ring conformations seen in the MARTINI force fields without affecting the general trends in conformation properties, which were already good in the MARTINI force fields. The BMW model, however, shows preferred formation of the solvent-separated pair between PEG monomers. This observation is consistent with the recent PMF calculation between uncharged solutes in the BMW,[34] which predicts global minimum at near 1 nm. We also show that the use of the polarizable MARTINI water model does not make much difference when compared to the standard noncharged MARTINI water.

Atomistic PEG in bundled SPC water molecules also shows a ring-like conformation, suggesting that the rings seen in the MARTINI force field are a direct consequence of a bundling of the water molecules. In this regard, the BMW model behaves rather like an unbundled water cluster, although the observed solvent-separated ring conformation reflects its own artifact.

The use of a CG site to represent four water molecules is appealing because of the enormous savings in computational time. The solvent is often not of interest, and an approximate treatment is desirable. Implicit solvent models have been shown to introduce artifacts, when applied to polymer solutions. Furthermore, devising implicit solvent models for semidilute solutions is difficult because it is not clear how one treats isolated pockets of solvent. Highly coarse-grained explicit solvent models therefore offer the promise of realistic results with large computational savings.

The simulations emphasize some pitfalls in coarse-graining several molecules into a single site and also suggest the properties of polymers might be a stringent test for CG force fields. The MARTINI and BMW force fields have been shown to be successful for a variety of problems, but few of those involved large-scale conformational changes as seen in polymers. This work points out that merely bundling water can result in artifacts that are easily seen in polymer simulations but not in biophysics applications.

AUTHOR INFORMATION

Corresponding Author

*Tel.: (608) 262-0258. E-mail: yethiraj@chem.wisc.edu.

Present Address

[§](J.M.) Department of Chemistry, Columbia University, New York 10027, United States.

Notes

The authors declare no competing financial interest.

ACKNOWLEDGMENTS

This material is based upon work supported by the National Science Foundation under Grant No. CHE-1111835. We are grateful for generous computational support from trestles and gordon machine in the San Diego Supercomputer Center (SDSC) under grant number TG-CHE090065 and the UW Madison Chemistry Department cluster Phoenix under grant number CHE-0840494. We also thank Dr. Hwankyu Lee for providing us with atomistic simulation data.

REFERENCES

(1) Harris, J. M.; Chess, R. B. Effect of Pegylation on Pharmaceuticals. *Nat. Rev. Drug Discovery* **2003**, *2*, 214−221.

(2) Davis, G. R.; Santa Ana, C. A.; Morawski, S. G.; Fordtran, J. S. Development of a Lavage Solution Associated with Minimal Water and Electrolyte Absorption or Secretion. *Gastroenterology* **1980**, *78*, 991−995.

(3) Tokuriki, N.; Kinjo, M.; Negi, S.; Hoshino, M.; Goto, Y.; Urabe, I.; Yomo, T. Protein Folding by the Effects of Macromolecular Crowding. *Protein Sci.* **2004**, *13*, 125−133.

(4) Ai, X.; Zhou, Z.; Bai, Y.; Choy, W. 15N NMR Spin Relaxation Dispersion Study of the Molecular Crowding Effects on Protein Folding Under Native Conditions. *J. Am. Chem. Soc.* **2006**, *128*, 3916−3917.

(5) Albertsson, P.-Å. *Partition of Cell Particles and Macromolecules*, 3rd ed.; Wiley: New York, 1986.

(6) Vincent, B.; Luckham, P. F.; Waite, F. A. The Effect of Free Polymer on the Stability of Sterically Stabilized Dispersions. *J. Colloid Interface Sci.* **1980**, *73*, 508−521.

(7) Ohshima, Y. N.; Sakagami, H.; Okumoto, K.; Tokoyoda, A.; Igarashi, T.; Shintaku, K. B.; Toride, S.; Sekino, H.; Kabuto, K.; Nishio, I. Direct Measurement of Infinitesimal Depletion Force in a Colloidal-Polymer Mixture by Laser Radiation Pressure. *Phys. Rev. Lett.* **1997**, *78*, 3963−3966.

(8) Saeki, S.; Kuwahara, N.; Nakata, M.; Kaneko, M. Upper and Lower Critical Solution Temperatures in Poly (ethylene glycol) Solutions. *Polymer* **1976**, *17*, 685−689.

(9) Spitzer, M.; Sabadini, E.; Loh, W. Poly(ethylene glycol) or Poly(ethylene oxide)? Magnitude of End-Group Contribution to the Partitioning of Ethylene Oxide Oligomers and Polymers Between Water and Organic Phases. *J. Braz. Chem. Soc.* **2002**, *13*, 7−9.

(10) Lee, H.; Vries, A. H.; Marrink, S.; Pastor, R. A Coarse-Grained Model for polyethylene oxide and polyethylene glycol: Conformation and hydrodynamics. *J. Phys. Chem. B* **2009**, *113*, 13186−13194.

(11) Rossi, G.; Fuchs, P. F. J.; Barnoud, J.; Monticelli, L. A Coarse-Grained MARTINI Model of Polyethylene Glycol and of Polyoxyethylene Alkyl Ether Surfactants. *J. Phys. Chem. B* **2012**, *116*, 14353−14362.

(12) Lee, H.; Venable, R. M.; MacKerell, A. D., Jr.; Pastor, R. Molecular Dynamics Studies of Polyethylene Oxide and Polyethylene Glycol:Hydrodynamic Radius and Shape Anisotropy. *Biophys. J.* **2008**, *95*, 1590−1599.

(13) Lee, H.; Pastor, R. W. Coarse-Grained Model for PEGylated Lipids: Effect of PEGylation on the Size and Shape of Self-Assembled Structures. *J. Phys. Chem. B* **2011**, *115*, 7830−7837.

(14) Wu, Z.; Qiang, C.; Yethiraj, A. A New Coarse-Grained Model for Water: The Importance of Electrostatic Interactions. *J. Phys. Chem. B* **2010**, *114*, 10524−10529.

(15) Pronk, S.; Pall, S.; Schulz, R.; Larsson, P.; Bjelkmar, P.; Apostolov, R.; Shirts, M. R.; Smith, J. C.; Kasson, P. M.; Van der Spoel, D.; Hess, B.; Lindahl, E. GROMACS 4.5: A High-Throughput and Highly Parallel Open Source Molecular Simulation Toolkit. *Bioinformatics* **2013**, *29*, 845−854.

(16) Berendsen, H. J. C.; Postma, J. P. M.; van Gunsteren, W. F.; Hermans, J. Interaction Models for Water in Relation to Protein Hydration. *Intermolecular Forces*; Reidel: Dordrecht, 1982.

(17) Berendsen, H. J. C.; Postma, J. P. M.; DiNola, A.; Haak, J. R. Molecular Dynamics with Coupling to an External Bath. *J. Chem. Phys.* **1984**, *81*, 3684−3690.

(18) Darden, T.; York, D.; Pedersen, L. Particle Mesh Ewald: An Nlog(N) Method for Ewald Sums in Large Systems. *J. Chem. Phys.* **1993**, *98*, 10089−10092.

(19) Essmann, U.; Perera, L.; Berkowitz, M. L.; Darden, T.; Lee, H.; Pedersen, L. G. A Smooth Particle Mesh Ewald Potential. *J. Chem. Phys.* **1995**, *103*, 8577−8592.

(20) Fuhrmans, M.; Sanders, B. P.; Marrink, S.; Vries, A. H. Effects of Bundling on the Properties of the SPC Water Model. *Theor. Chem. Acc.* **2010**, *125*, 335−344.
(21) Martin, M. G.; Siepmann, J. I. Transferable Potentials for Phase Equilibria. 1. United-Atom Description of n-Alkanes. *J. Phys. Chem. B* **1998**, *102*, 2569−2577.
(22) Hezaveh, S.; Samanta, S.; Milano, G.; Roccatano, D. Structure and Dynamics of 1,2-Dimethoxyethane and 1,2-Dimethoxypropane in Aqueous and Non-Aqueous Solutions: A Molecular Dynamics Study. *J. Chem. Phys.* **2011**, *135*, 164501.
(23) Hezaveh, S.; Samanta, S.; Milano, G.; Roccatano, D. Synthetic Polymers and Biomembranes. How Do They Interact?: Atomistic Molecular Dynamics Simulation Study of PEO in Contact with a DMPC Lipid Bilayer. *J. Phys. Chem. B* **2006**, *110*, 26170−26179.
(24) Dormidontova, E. E. Influence of End Groups on Phase Behavior and Properties of PEO in Aqueous Solutions. *Macromolecules* **2004**, *37*, 7747−7761.
(25) Marrink, S. J.; Risselada, H. J.; Yefimov, S.; Tieleman, D. P.; de Vries, A. H. The MARTINI Force Field: Coarse Grained Model for Biomolecular Simulations. *J. Phys. Chem. B* **2007**, *111*, 7812−7824.
(26) Yesylevskyy, S. O.; Schafer, L. V.; Sengupta, D.; Marrink, S. J. Polarizable Water Model for the Coarse-Grained MARTINI Force Field. *PLoS Comput. Biol.* **2010**, *6*, e1000810.
(27) Striolo, A.; McCabe, C.; Cummings, P. T. Effective Interactions Between Polyhedral Oligomeric Sislesquioxanes Dissolved in Normal Hexadecane from Molecular Simulation. *Macromolecules* **2005**, *38*, 8950−8959.
(28) Jorgensen, W. L.; Maxwell, D. S.; Tirado-Rives, J. Development and Testing of the OPLS All-Atom Force Field on Conformational Energetics and Properties of Organic Liquids. *J. Am. Chem. Soc.* **1996**, *118*, 11225−11236.
(29) Briggs, J. M.; Matsui, T.; Jorgensen, W. L. Monte Carlo Simulations of Liquid Alkyl Ethers with the OPLS Potential Functions. *J. Comput. Chem.* **1990**, *11*, 958−971.
(30) Ren, C. L.; Tian, W. D.; Szliefer, I.; Ma, Y. Q. Specific Salt Effects on Poly(ethylene oxide) Electrolyte Solutions. *Macromolecules* **2011**, *44*, 1719−1727.
(31) Wu, Z.; Cui, Q.; Yethiraj, A. Driving Force for the Association of Hydrophobic Peptides: The Importance of Electrostatic Interactions in Coarse-Grained Water Models. *J. Phys. Chem. Lett.* **2011**, *2*, 1794−1798.
(32) Wu, Z.; Cui, Q.; Yethiraj, A. A New Coarse-Grained Force Field for Membrane-Peptide Simulations. *J. Chem. Theory Comput.* **2011**, *7*, 3793−3802.
(33) Frielinghaus, H.; Pedersen, W. B.; Larsen, P. S.; Almdal, K.; Mortensen, K. End Effects in Poly(styrene)/Poly(ethylene oxide) Copolymers. *Macromolecules* **2001**, *34*, 1096−1104.
(34) Wassenaar, T. A.; Ingólfsson, H. I.; Prieß, M.; Marrink, S. J.; Schäfer, L. V. Mixing MARTINI:Electrostatic Coupling in Hybrid Atomistic-Coarse-Grained Biomolecular Simulations. *J. Phys. Chem. B* **2013**, *117*, 3516−3530.
(35) Humphrey, W.; Dalke, A.; Schulten, K. VMD-Visual Molecular Dynamics. *J. Mol. Graphics* **1996**, *14*, 33−38.